

NeuroPlug: Plugging Side-Channel Leaks in NPUs using Space Filling Curves

Nivedita Shrivastava
Dept. of Electrical Engineering
Indian Institute of Technology Delhi
New Delhi, India
nivedita.shrivastava@ee.iitd.ac.in

Smruti R. Sarangi
Dept. of Electrical Engineering
Indian Institute of Technology Delhi
New Delhi, India
srsarangi@cse.iitd.ac.in

Abstract—Securing deep neural networks (DNNs) from side-channel attacks is an important problem as of today, given the substantial investment of time and resources in acquiring the raw data and training complex models. All published countermeasures (CMs) add noise N to a signal X (parameter of interest such as the net memory traffic that is leaked). The adversary observes $X+N$; we shall show that it is easy to filter this noise out using targeted measurements, statistical analyses and different kinds of reasonably-assumed side information. We present a novel CM *NeuroPlug* that is immune to these attack methodologies mainly because we use a different formulation $CX + N$. We introduce a multiplicative variable C that naturally arises from feature map compression; it plays a key role in obfuscating the parameters of interest. Our approach is based on mapping all the computations to a 1-D space filling curve and then performing a sequence of tiling, compression and binning-based obfuscation operations. We follow up with proposing a theoretical framework based on Mellin transforms that allows us to accurately quantify the size of the search space as a function of the noise we add and the side information that an adversary possesses. The security guarantees provided by *NeuroPlug* are validated using a battery of statistical and information theory-based tests. We also demonstrate a substantial performance enhancement of 15% compared to the closest competing work.

I. INTRODUCTION

Deep neural network (DNN) models embody a significant amount of intellectual property (IP). Creating such models requires a massive amount of investment in terms of financial resources and human effort: data collection via mechanical turks, model design and rigorous training [61], [62]. Attackers thus have a very strong incentive to steal the model parameters associated with these DNN models such as the nature/number of layers, details of weights, etc. [61], [62]. Such security breaches can potentially compromise the privacy, security and integrity of large autonomous systems. For example, an attacker can make a small human-invisible change to lane markings or traffic lights, which are sufficiently powerful to confuse lane detection and traffic light sensing models, respectively [49], [69], [72]. Possessing even partial knowledge about the inner workings of a DNN model significantly enhances the feasibility of orchestrating successful attacks – adversarial attacks [39], membership inference attacks [41] and bit-flip attacks [75].

For the last 5 years, attackers and defenders have been locked in an arms race to design more potent attacks and

countermeasures (CMs), respectively. The attacker relies on a memory/timing based side channel that leaks a signal X , which carries a lot of information about the aforementioned model parameters. X could be the number of off-chip bytes transferred (*volume*), computational *time*, the number of bytes read between a write→read to the same memory address (read-write *distance*), the number of times a byte is read (*count*), or any combination thereof. Existing countermeasures (CMs) present $Y = X + N$ to the attacker, where N is the added noise. State-of-the-art attacks [27], [29], [73], [74] look at a subset of these four variables – count, distance, time and volume (CDTV) – and try to reduce the search space of X by collecting multiple measurements and using specially crafted inputs. On the other hand, CMs use a combination of shuffling data, adding dummy accesses and on-chip buffering to hide the noise parameter.

Shortcomings of Current CMs The most relevant, state-of-the-art CMs are shown in Table I (details in Section II). Given that X is a constant for a given layer as the model parameters will remain the same, repeated measurements with possibly different inputs and possibly across multiple devices shall yield the distribution of N . If the mean of N is 0 or the minimum is 0, then the noise gets effectively filtered out (*statistical (SS) attack*) ([40], [53]). Assume that this is not the case, then any measurable statistical metric is a non-zero constant N_c , which is typically a hardwired value [9]. Any such hardwired value can be leaked by a malicious insider [1], [55], [56], [60]. It also violates the Kerckhoff’s principle [32], which clearly states that security cannot be derived from hiding aspects of the design.

Such *Kerckhoff (KK) attacks* can yield all the constants that characterize the parameters of the noise distribution and this leads to an estimate of X . Now, assume that despite statistical and Kerckhoff attacks, our search space is still large. We can then glean some knowledge from sister neural networks (belonging to the same genre) and try to make educated guesses. For instance, layer sizes are mostly multiples of squares (see [9], [29]). Such numbers are formally known as non-square-free (NSQF) numbers [48]. With other reasonable assumptions regarding layer skewness, our search space can reduce drastically. Let us refer to this as a side-information (SI) attack.

Countermeasure	Protects				Security Metric			Perf. metric	Counterattacks	Leakage
	Count	Distance	Time	Volume	SrS.	Accu.	Theo.			
Liu et al. [40]	○	○	○	●	●	○	○	●	Statistical (§ III-1)	RW Dependencies
NPUFort [70]	○	○	●	○	○	○	○	●	Side-infor. (§ III-3)	Mem. access pattern
NeuroObfus. [38]	●	○	○	●	○	●	○	●	Statistical (§ III-2)	Mean noise
Zuo et al. [80]	○	○	●	○	○	●	○	●	Side-infor. (§ III-3)	Mem. access pattern
ObfuNAS [78]	●	○	○	●	○	●	○	●	Statistical (§ III-2)	Mean noise
DNNcloak [9]	●	●	○	●	○	●	○	●	Side-infor. (§ III-3) Kerckhoff (§ III-2)	Values of RWs Buffer size
NeuroPlug	●	●	●	●	●	●	●	●	-	-

TABLE I: *NeuroPlug* offers comprehensive protection and undergoes thorough validation using various security metrics. ● property is satisfied and ○ means it is not. **SrS.** is the search space, **Accu.** is model re-training accuracy or how accurately the layer parameters are estimated. **Theo.** refers to information-theory based security metrics.

Using these three attacks – SS, KK and SI – we were able to break all the CMs mentioned in Table I. Breaking these approaches required a maximum of 60,000 runs. If the real fabricated NPUs were available (7nm technology), we estimate the process to take a maximum of 8-10 hours. Using layer-based obfuscation approaches (dynamically fuse/split layers) [38] did not prove to be very useful other than enlarging the search space moderately, primarily because it does not fundamentally obfuscate the CDTV metrics.

Our Insights We introduce a new degree of freedom by augmenting the $X + N$ formulation with a multiplicative random variable C . The new formulation becomes an affine transform of the form $CX + N$. We shall show in Section VI that for our proposed design *NeuroPlug*, this formulation increases the search space by roughly 10^{70} times after filtering out as much of the noise as we can (using the SS, KK and SI attacks). This is the bedrock of our design.

Our Solution: *NeuroPlug* This factor C naturally arises from data compression in our design and can further be augmented by adding custom noise. Insofar as the adversary is concerned, all the CDTV metrics are affected to different extents because of compression – the effect is equivalent to reading and writing CX bytes. To enable data compression as an obfuscatory tool, we need to represent a computation in a DNN differently. This choice segues into the novel notion of using 1-D space filling curves (SFCs) [57] to map a complex 3-D space of DNN computations to an equivalent 1-D space. This 1-D curve conceptually snakes through all the computation layers of a DNN (possibly with skip connections) and allows us to create contiguous chunks of bytes (tiles), compress them and bin them.

A *tile* can be split across bins and we can also leave space within a bin empty (contribution to the N in $CX + N$). Now, C is tied to the plaintext. Many may argue that given that the plaintext is known, it is possible to estimate C , at least in the first few layers. In the later layers due to both aleatoric (inherent) and epistemic (lack of knowledge of model parameters) uncertainty, estimating C is difficult [21]. Hence, in the first few layers, we need to enhance the uncertainty in the noise N and also add some random text in the data to obfuscate C . Plaintext-aided encryption is known to work well with such safeguards [10], [16], [64]. Now, to not run

afoul of the SS and KK attacks, we make these dummy text snippets and all the parameters that determine the nature of the noise distribution N a part of the *key* (the encrypted DNN model in this case). This is allowed. This ensures that even if the key is compromised, the effects will be limited to systems that use the key. The key can always be changed (refer to the paper on secure leasing [34]).

Figure 1 shows the outline of our scheme. The SFC and the affine transform ($CX + N$) are the central themes, which lead to an architecture based on tiling, binning, compression and noise addition. Regardless of the side-information available, we show that introducing the extra degree of freedom (C) has a dramatic effect on the search space, whose size is computed using our novel Mellin transform [15] based framework. Given that we can modulate C by adding random noise, the size of the search space can be increased (at the cost of performance). This may be required in the future if the model owner desires greater levels of protection or the HW becomes faster. To the best of our knowledge, such a systematic and mathematically grounded approach of search space estimation is novel. Note that the size of the search space yielded by our analysis is a function of the side information possessed by the adversary. The adversary is limited to only memory and timing-based side channels.

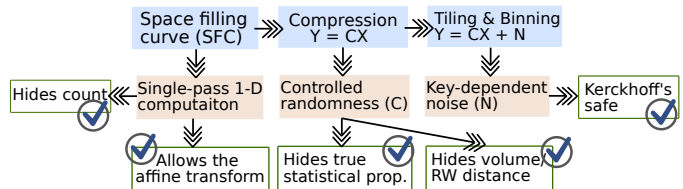


Fig. 1: The overall scheme

The specific **list of contributions in this paper** is as follows: ① A comprehensive experimental study of the information leaked regarding input/output feature dimensions by sister NNs. ② A thorough analysis of the limitations in existing state-of-the-art security solutions in the light of recent threats – SS, KK and SI attacks. ③ A formal theoretical framework to quantify the “smart” search space in the system given a bound on the information leaked to the adversary. ④ A novel approach to enhance the security of NN accelerators hiding the

leaked signatures using an SFC-based execution pattern. ⑤ A detailed theoretical and performance analysis of *NeuroPlug*, which shows a 15% performance improvement over the closest competing work (*DNNcloak*). ⑥ Two case studies of state-of-the-art attacks on sparse and dense accelerators (resp.), a rigorous evaluation based on computing the size of the search space for a given amount of added noise (and side information), a performance-security trade-off analysis, and thorough statistical and information theory-based tests. §II provides the background and outlines the threat model. §III provides the motivation. §IV provides a theoretical description of the proposed scheme. §V presents the proposed design, §VI and §VII present the performance and security analyses, respectively. §VIII presents the related work. We finally conclude in §IX.

II. BACKGROUND AND THREAT MODEL

A. Convolution Neural Networks (CNNs)

Convolution serves as the core component of a DNN. To process a layer, we sequentially traverse the input and output feature maps (referred to *ifmaps* and *ofmaps*, respectively), and apply the convolution operation. The K *ofmaps*, each of size $(P \times Q)$ are generated by convolving a filter of size $(R \times S)$ with C *ifmaps*. Each *ifmap*'s size is $H \times W$. For the sake of explanation, we assume that the *ofmap* and *ifmap* have the same dimensions $(P = H; Q = W)$ (refer to Table II).

Due to the limited on-chip storage, the elements in an *ifmap*, an *ofmap*, and a filter are often grouped into *tiles* [52] as shown in Listing 1.

```

1 // Off-chip
2 for (ko=0; ko<K; ko+=Tk) // K: #output fmaps
3   for (co=0; co<C; co+=Tc) // C: #input fmaps
4     for (ho=0; ho<H; ho+=Th) // H: #rows in a fmap
5       for (wo=0; wo<W; wo+=Tw) // W: #cols in a fmap
6         // On-chip
7         for (k=ko; k<ko+Tk; k++) // Tile level processing
8           for (c=co; c<co+Tc; c++)
9             for (h=ho; h<ho+Th; h++)
10              for (w=wo; w<wo+Tw; w++)
11                for (r=0; r<R; r++) // R: #rows in a filter
12                  for (s=0; s<S; s++) // S: #cols in a filter
13                    ofmap[k][h][w]+=ifmap[c][h+r][w+s] *
                      weights[k][c][r][s];

```

Listing 1: A basic convolution operation

Sym.	Notation	Sym.	Notation
K	#ofmaps	T _k	Tiling factor for # ofmaps
C	#channels	T _c	Tiling factor for # ifmaps
H/W	#rows/cols in an ifmap	T _h /T _w	Tiling factor for rows/cols
R/S	#rows/cols in a filter	P/Q	#rows/cols in a filter
β	Compression ratio	α	Additive noise

TABLE II: Glossary of the symbols

B. System Design and Threat Model

Our threat model reflects a scenario where a DNN model is performing inference tasks locally on an NPU using a pre-trained model. We present the high-level system design and threat model in Figure 2 (similar to previous attacks and CMs [29], [38], [74]).

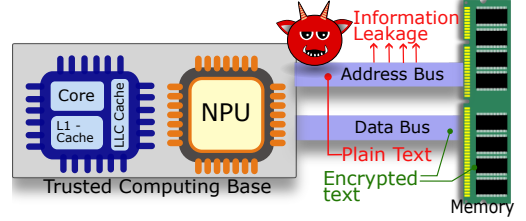


Fig. 2: The system design and the threat model (similar to [29], [38], [74]). An adversary snoops the address and the data buses to infer the memory access patterns.

We assume that the system consists of a central processing unit (CPU), NPU and caches. The CPU sends commands to the NPU through a *secure* channel. Like prior work, all transfer of data between the CPU and NPU takes place via main memory. The data in the main memory is encrypted and tamper-proof (using [62]). We assume the existence of a trusted execution environment (TEE) like Intel SGX [13], which is used to download the secure model and get the decryption key via a trusted third-party attestation based mechanism (refer to [59]). It can also periodically renew the model and the key using secure leasing [34]. The NPU, CPU, caches and the TEE are all within the trusted computing base (standard design decision: [28], [37], [62]).

Potential adversaries might include the operating system, the hypervisor, a malevolent application, or somebody having physical access to the main memory or memory bus.

Attacker's Aim The primary objective of an adversary is to reverse-engineer the architecture of the DNN model in order to facilitate subsequent attacks, including adversarial attacks and membership inference. She can also aim to retrain a comparable model with enhanced or similar accuracy.

Attacker's Capabilities and Limitations We assume a strong attacker, who can target the system memory and memory interface. She can craft specialized inputs and feed them to the accelerator. The adversary possesses the ability to read the memory addresses that are sent as plaintext on the memory bus and identify the type of memory access instruction (read or write). She can also monitor the transfer of encrypted data to/from DRAM memory. She however cannot tamper with the addresses or the encrypted data, or mount replay attacks (this can be ensured via Securator [62]). She can also use a high-resolution timer to track the timing between memory accesses. Then, she can mount SS, KK and SI attacks. This means that a model can be run any number of times with the same or different inputs and it can be run on as many devices as needed (to thwart CMs that use PUFs [47]). The attacker has full access to all hardwired parameters and the design of the NPU. Finally, the attacker has access to all contemporary DNN models and has learnt whatever it could from them. This information can be leveraged to mount SI attacks (we will quantify this in Section IV).

We do not consider power, thermal and EM-based attacks. Cache based attacks are not relevant here because the CPU's cache hierarchy is not used.

C. State-of-the-art Attacks and Countermeasures (CMs)

An attack aims to find the parameters for each CNN layer: size, width, height, number of *ifmaps* (input channels) and *ofmaps* (output channels). Reading a fully-computed *ofmap* signifies the termination of the preceding layer that produced it. This helps the adversary identify layer boundaries. There is a RAW dependency here (across layers) that is characterized by the write-to-read *distance* (bytes accessed between a write and the corresponding read). This is indicative of the layer size. Next, note that the same *ifmap* is used to generate different *ofmaps* using a plurality of filters. This means that the same datum is accessed several times (non-zero *count*): this leaks information regarding the number of *ofmaps*. Finally, note that every single byte of an *ifmap* is read by a layer – the total data volume (*volume*) that is read is indicative of the number of *ifmaps*. In fact, using these insights it is possible to setup a system of equations and solve them to find all the layer parameters (see [29]).

Since the filters are read-only and never modified, the attacker can easily distinguish between filter memory accesses and *ifmap/ofmap* accesses. This leaks the size of the filter. In addition to tracking off-chip traffic, an adversary can monitor the execution *time* of different modules [73] to establish a correlation between the dimensions of the model and the timing [73]. A recent attack *HuffDuff* [74] proposes a method to craft specialized inputs such that the total data volume of non-zero values leaks the filter sizes. They use a series of inputs that have one 1 and the rest 0s.

Countermeasures - Recent works [9], [38], [40] have proposed a set of obfuscation strategies to conceal these leaked signatures. They propose to shuffle accesses, widen the convolution layer by padding zeros, increase the dimensions of the filters, augment the input with dummy data/zeros, buffer a part of the *ofmap* or fuse/split layers. All of these methods increase the model search space but fail to hide important signals such as the access count or read-after-write dependence information (also pointed out in HuffDuff [74]).

III. MOTIVATION

1) *1st Generation Statistical Attack (SS)*: Attackers can always collect multiple measurements across various runs, inputs and devices, and perform sophisticated analyses. As long as doing this is practically feasible, it will continue to be a method of choice because these attacks are easy to mount.

For instance, when adding dummy writes (redundancy based noise [40]) in a system, it is necessary to read the dummy data, and then write something back. Otherwise, it is obvious that the original data is ineffectual. Figure 3 shows an example of a CM [40] that had this vulnerability and a method to detect and eliminate such writes.

On similar lines, *shuffling* the addresses [40] will also prove to be ineffective, as they also preserve the average read-write (RW) distance [9].

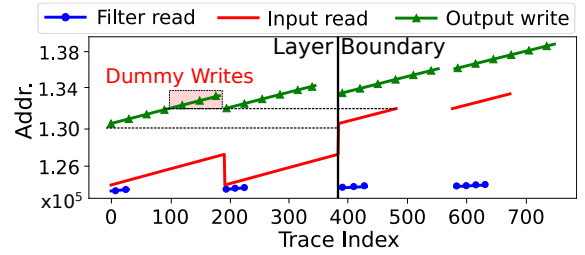


Fig. 3: SS attack: Adding dummy writes (784) to obfuscate the true writes (1568) in the scaled version of the first layer of *Vgg16* ($32 \times 32 \times 3$). Adversaries eliminate the dummy writes as they are not read in the subsequent layer (Liu et al. [40])

Can we stop statistical attacks?

The adversary will estimate the pattern in the leaked data or parameters of the noise distribution by analyzing multiple samples collected over space and time.

2) *2nd Generation Kerckhoff Attack (KK)*: It is possible that even after collecting multiple samples, an adversary cannot filter out the noise or estimate parameters of the distribution such as the value of the non-zero mean or the minimum. The *2nd generation Kerckhoff* attacks are built over the *1st generation attacks* to leak such hardwired parameters. It is possible for a malicious insider to leak them in accordance with the Kerckhoff’s principle.

Some popular approaches [38], [78] obfuscate the layer size by adding dummy accesses (*redundancy in space*), while *DNNCloak* [9] removes the accesses by buffering the data on-chip (*removal*). Let us assume that the size of the layer is X and the noise is N . To counter this, an adversary first conducts a statistical attack by collecting a multitude of data samples. They will converge to the mean as per the law of large numbers (shown in Figure 4). In this case, the noise added is 22400, which is a hardwired constant and can be leaked. Even if it is tied to the plaintext or the hardware (via PUFs [47]), taking multiple samples will ultimately produce the mean and the minimum (the most useful parameters).

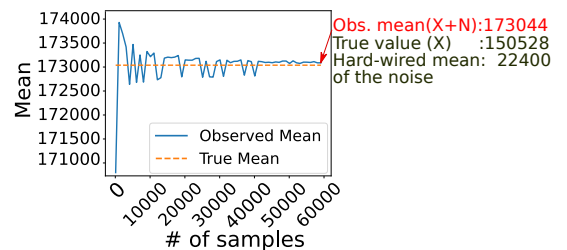


Fig. 4: KK attack: A noise with a hardwired mean value of 22400 is added to obfuscate the actual volume of the first layer of *Vgg16* ($224 \times 224 \times 3$) [38], [78]. The adversary will eliminate the noise using an SS attack followed by the *Kerckhoff*’s (KK) attack

Do not violate the *Kerckhoff* principle

Any hardcoded secret parameter or constant may be leaked by a *malicious insider*.

There is always a residual side-channel

An adversary can collect side-information from contemporary DNNs and use it to estimate the parameters of the target model and reduce the search space.

3) *3rd Generation Residual Side-channel Attack (SI)*: To circumvent the KK attack, we can make many of the hardcoded constants a part of the *key*. The advantage of this method is that a malicious insider cannot leak them, and the key can be changed as frequently as we want (see [34]). An adversary always has some idea of the nature of the neural network that is being used based on what she knows from prior work and the nature of the problem that is being solved – it would be unwise to assume otherwise. This information can be weaponized.

Consider the example shown in Figure 5. It shows an execution snippet from DNNCloak (Che et al. [9]). Here, a layer is split into sublayers and dummy accesses are added to the sublayers. The idea is to read the output of the previous sublayer into the current sublayer and write the output of both the sublayers simultaneously (current and previous). This is done with the hope that dummy writes cannot be filtered out because they are read and used in the next sublayer – artificial RAW dependencies are being created as everything that is being written is being read. The adversary can *check* the contents of the addresses that are getting updated. As shown in the figure, it is easy to spot that the values of some addresses that do not get updated. This will still be the case even if the data as well as the addresses are encrypted with the same key. Based on an analysis of access patterns in state-of-the-art DNNs, any adversary will know that the occurrence of this phenomenon is highly unlikely and thus they are dummy writes in all likelihood. Even if we shuffle the addresses, this pattern can still be discerned for individual blocks of addresses.

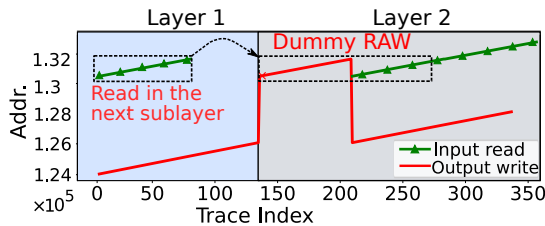


Fig. 5: SI attack: Layer divider technique [9] to obfuscate RAW dependencies. The adversary filters out the fake RAW dependencies by checking the unchanged values.

To reduce the search space, we can use another trick. We analyzed all the contemporary neural networks. By and large, each layer is of the form $M^2 \times N$, where M is a large integer and N is comparatively smaller for the first few layers. Such numbers are known as NSQF (non square-free) numbers. If we only consider NSQF numbers [48] with a set of constraints derived from layers’ dimensions in contemporary DNNs, the search space can reduce considerably.

IV. THEORETICAL ANALYSIS

Consider a random variable Y , which corresponds to the number of tiles that the attacker *observes* for a given layer. This is related to the actual number of tiles X , the compression ratio C and the amount of noise N as $Y = CX + N$.

Given that C is a compression ratio, the following constraint holds: $0 < C \leq 1$. The aim is to arrive at X from Y .

A. The Additive Noise: N

Any adversary would like to reduce the degrees of freedom and keep C constant such that the effect of the noise N (dummy data) can be eliminated. This can be ensured by making minor changes to the input such that the neural network’s layers effectively filter them out. For example, we can add speckled noise that does not correspond to any identifiable feature [79]. Multiple measurements will yield $CX + N_{min}$. Here, N_{min} is the minimum value that N can take. If N_{min} is known (as per the *Kerckhoff*’s principle), then CX is exposed.

If an adversary can estimate C (based on prior studies), the system’s security is compromised. We can substitute N_{min} with any other statistical metric like the mean or variance – it does not make a difference. As we discovered in our experimental analyses, tying N to the model input or PUFs does not significantly help because it is possible to collect a distribution of N anyway by running experiments on multiple devices or using different model inputs [6], [7].

For the sake of explanation, let us use N_{min} as the metric of interest. To make a significant difference, it should not be derived from the model input, it cannot be zero and it definitely cannot be *known*. If it arises from a distribution, then we shall continue to have the same problem. The only “Kerckhoff safe” approach is to make the parameters that govern N ’s distribution like N_{min} a part of the *key* (encrypted model in our case).

Even if N_{min} is a part of the key, we are still allowing the attacker to guess it with a finite number of choices. Hence, it is a good idea to create a distribution on top of it just to increase the computational difficulty. Let us thus modify our equation as $Y = CX + \alpha + N'$. In this case, α is a constant (should be a part of the key, proxy for N_{min}) and N' is a distribution whose support is from 0 till R , where R along with the parameters of the distribution should also be a part of the key. Let us again give the adversary the benefit of doubt, and assume that she can isolate measurements where $N' = 0$. In this case, $Y = CX + \alpha$.

B. The Multiplicative Noise: C

Let us assess the difficulty of guessing C . Assume that the adversary knows some distribution of C ($f(C)$) for a given layer (learnt from other DNNs). Let us give the adversary

the benefit of doubt and assume that she knows when a layer begins and ends.

Having some knowledge of $f(C)$ gives a good starting point to search for X . The problem is finding the actual compression ratio β . In this case, $Y = \beta X + \alpha$. Unlike the noise N , statistical and *Kerckhoff* attacks are hard to mount on the compression ratio mainly because of two reasons. The first is that it cannot be a hardwired constant and thus hardware designers will not know what the compression ratio for a given layer will be.

In the case of the additive noise, a standard approach is to conduct measurements using a diversity of inputs [6], [7] and find the mean or minimum value of $X+N$. With multiplicative noise of the form CX , an analogous metric is the geometric mean. It is not very helpful mainly because either C does not change with a perturbed input or it does not change in a way that is known to the attacker. The latter is because of *aleatoric* uncertainty, which comes from randomness in the data, and *epistemic* uncertainty, which arises from limited knowledge about the model. Because of these uncertainties, the only extra information that the attacker can have is a prior distribution $f(C)$ (learnt from other models that may be similar). This is side information and its quality depends on how well the model under attack is similar to known models in the literature. Note that C can always be modulated by the model creator by adding random dummy data in a layer. The amount of dummy data to be added can be a part of the key.

C. Predicted Distribution of X

The actual distribution of X is not known to the adversary. It however knows the following formula without knowing the values of α and β .

$$X = (Y - \alpha) \times \frac{1}{\beta} \quad (1)$$

Y is the value that the adversary observes, which in our design will be the DRAM traffic volume for compressed and then encrypted data. We are basically looking at a product of two random variables here. Let the random variable U denote $Y - \alpha$ and V denote $\frac{1}{\beta}$. We have:

$$X = UV \quad (2)$$

If we take the Mellin transform [4] of both sides, we get.

$$\mathcal{M}(X) = \mathcal{M}(UV) = \mathcal{M}(U) \times \mathcal{M}(V) \quad (3)$$

A Mellin transform is defined as:

$$g(s) = \mathcal{M}(f(x)) = \int_0^{\infty} x^{s-1} f(x) dx \quad (4)$$

The inverse transform is:

$$f(x) = \mathcal{M}^{-1}(g(s)) = \frac{1}{2\pi i} \int_{c-i\infty}^{c+i\infty} x^{-s} g(s) ds \quad (5)$$

Given a Y , an adversary can thus get a distribution of X using an estimate of the distributions of α and β ($f(C)$), and then by using *Mellin* transforms. Let us represent the adversary's predicted distribution by the pdf $h(X)$.

1) *Difficulty of Verification*: Given a distribution of X , the most optimal way of making guesses is to first choose the most probable value (supremum), then the second most probable value, and so on (see Massey [45] for the proof). Let us thus define the *rank* function that takes the adversary's predicted distribution $h(X)$ and the real value of X (X_r) as input. It sorts the values of X in descending order of their probabilities and returns the rank of X_r . For example, if X_r is the mode of the distribution, its rank is 1. Hence, we have a way of **quantifying the search space**. If there are N_i choices in layer i , then the total number of choices is $\prod_i N_i$. Note that layers' dimensions/parameters in this approach cannot be independently verified.

This creates an all-or-nothing scenario, requiring the verification of a predicted combination of dimensions for the entire neural network in one comprehensive step. This is done by training and verifying the accuracy of the predicted network.

2) *Imperfect Knowledge of $f(X)$* : The *Mellin* transform's computation involves approximating the integral using methods like the Riemann sum [15]. However, its quadratic complexity imposes limitations on its practical utility for extensive computations [15]. Sena et al. [15] proposes an alternative that uses the FFT to compute the *Mellin* transform. This is achieved by performing spline interpolation, exponential resampling, exponential multiplication followed by FFT computation.

The adversary uses this approach to estimate the distribution $h(X)$. Next, she performs an interpolation based on the *piecewise cubic hermite polynomial (PCHIP)* [76], to modify $h(X)$ such that the probability of all non-NSQF numbers is zero. Every NSQF number accumulates the probabilities of all the non-NSQF numbers in its neighborhood (half the distance on either side to the nearest NSQF number). This is our *smart search space* (probability distribution: $h'(X)$).

Rank Estimation We ran this experiment for estimating the rank of X (layer volume) for the first five layers of *Vgg16* (see Figure 6), where the true value of *ifmap* (X_r) for each layer is 150528, 802816, 401428, 802816, and 200704, respectively.

In order to estimate the side-information available to the adversary regarding the compression ratio, we studied the compression ratios for nine *cognate* open-source DNN models – *AlexNet* [33], *Vgg16* [63], *Vgg19* [63], *SqueezeNet* [30], *ShuffleNet* [77], *ResNet* [25], *MobileNet* [26], *GoogLeNet* [65] and *Inception Net* [66]. Based on the observed range of the compression ratios ($1.5\times - 40\times$) (also observed in [23]) across different DNN models (also pruned and quantized), we generate different distributions for U and V . We vary α between [100, $224 \times 224 \times 128$ (layer size)]. Next, we compute $h'(X)$ using our Mellin transform based approach. We observe that the uniform distribution has the highest rank of X_r followed by the geometric distribution.

V. DESIGN OF NEUROPLUG

A. Overview

The high-level design of *NeuroPlug* is shown in Figure 7. The host CPU securely delivers instructions to the NPU via a PCIe link to execute a layer of the DNN. Each layer is divided

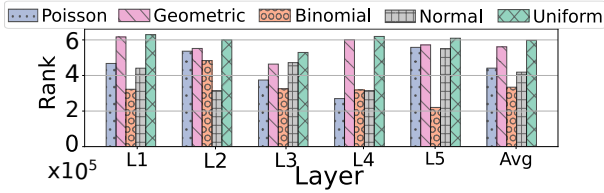


Fig. 6: Rank of X_r (layer volume) for different layers of Vgg16. From our point of view the uniform distribution is the best.

into a set of tiles (basic unit of computation). Subsequently, the NPU starts tile-wise computation of convolutions and other linear/nonlinear operations.

We map the complex multi-dimensional computation space of a DNN’s layer to a 1-D space using a SFC (space-filling curve). The SFC conceptually moves through all the tiles in a layer – first along the channels, then along the rows (see Listing 1). In the SFC, we compress a sequence of contiguous tiles and fit them in a *bin*, where all the bins have the same size. Tiles can be split across bins and we can also leave space empty within a bin. A *Bin Table* is stored at the beginning of a bin that stores the starting address of each compressed tile in a bin.

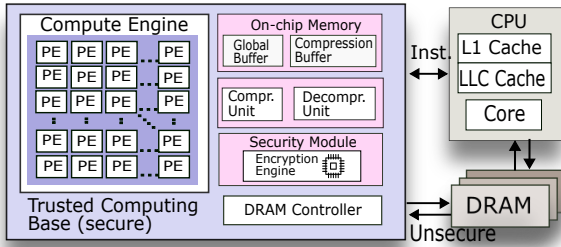


Fig. 7: The high-level design of NeuroPlug

The *bin* is the atomic unit of *storage* in our system, whereas a *tile* is the atomic unit of *computation*. A bin is read and written in one go. Furthermore, we ensure that it takes exactly the same amount of time to process each bin such that timing side-channels are plugged. We place a bound κ on the maximum number of tiles that can be stored within a bin – the processing time of a bin corresponds to processing all κ tiles (included in the calculation of performance overheads).

The compute engine is a traditional systolic PE array; each PE has local storage in the form of register files and local buffers and a tile decompression unit. As the *first layer is the most exposed*, we enhance its security by initially packing dummy data within the tiles before performing compression – its location is stored in the Bin Table.

A dedicated compression engine [23] compresses the tiles, packs them in bins, leaves some space empty (as per the noise distribution) and writes them in a sequential order to the main memory (as an SFC for the next layer). *This ensures that writes are also at the granularity of bins and follow the*

same semantics. SFCs provide a convenient abstraction for representing computations within a DNN along with providing performance benefits in the form of enhanced spatial locality.

B. Deep Look at SFC-based Computation

Let us analyze the computation patterns with SFCs (refer to Table II for the terminology). In a simplistic avatar of our design, we assume that all the *ifmaps* and weights fit on chip (will be relaxed later). The *ifmap* is stored as a simple 1-D SFC as shown in Figure 8(a). Each cuboid represents a *deep tile* – same tile across all the input channels. We start with the first deep tile (iterate across all the channels) and then move to the next deep tile in the same row and so on. Once we finish processing a row, we move to the next row (first column), so on and so forth. The weights are also stored as an SFC. A single 1-D SFC contains CK kernels – we first read all the weights to generate *ofmap* 1, then *ofmap* 2, so on and so forth (refer to Figure 8(b)). The *ofmaps* have exactly the same format as *ifmaps*– this needs to be the case because they are inputs to the next layer. Refer to Figure 8(c) that shows the order in which we write. Table III outlines the key design principles using SFCs. Let us now make our design more realistic.

- ▶ Read/write an *ifmap* or *ofmap* only once.
- ▶ Read all the channels of an *ifmap* tile together (a deep tile).

TABLE III: Design principles

1) **Case I:** *Weights do not fit but input maps do:* Consider the case where the weights do not fit in the NPU memory buffers but the inputs do. In this case, we partition the weights on the basis of a partitioning of *ofmaps*. This is akin to partitioning the set of K *ofmaps* into a sequence of contiguous subsets of k_1, k_2, \dots, k_n *ofmaps* where $\sum_{i=1}^n k_i = K$. In practice, this is not visible to the attacker because we read the filters for the first k_1 *ofmaps* and compute them fully, then do the same for the next k_2 , up till k_n . The *ofmaps* are stored one after the other – exactly in the same format as they would have been stored had all the weights fit in memory. The timing of filter reads could be a side-channel, however, we obscure this by ensuring that each bin takes a fixed amount of time to execute and the inter-bin and inter-filter-bin read time is the same.

2) **Case II:** *Input maps do not fit but weights do:* We split an *ifmap* bin-wise such that each set of bins fits within the NPU (row-major order). Then the deep tiles in each set of bins are processed and the corresponding output tiles/bins are written to memory. This is indistinguishable from the case in which all inputs and weights fit in on-chip memory.

3) **Case III:** *Both inputs and weights do not fit:* We partition an *ifmap*’s SFC bin-wise such that each partition fits within the NPU. Then we proceed on the lines of Case I (single pass through all the weights). We need to subsequently read the next set of *ifmap* bins and re-read all the filters once again. This is where a side-channel gets exposed. The frequency at which the same filter weights are read correlates directly with the total volume of input data. A straightforward solution is

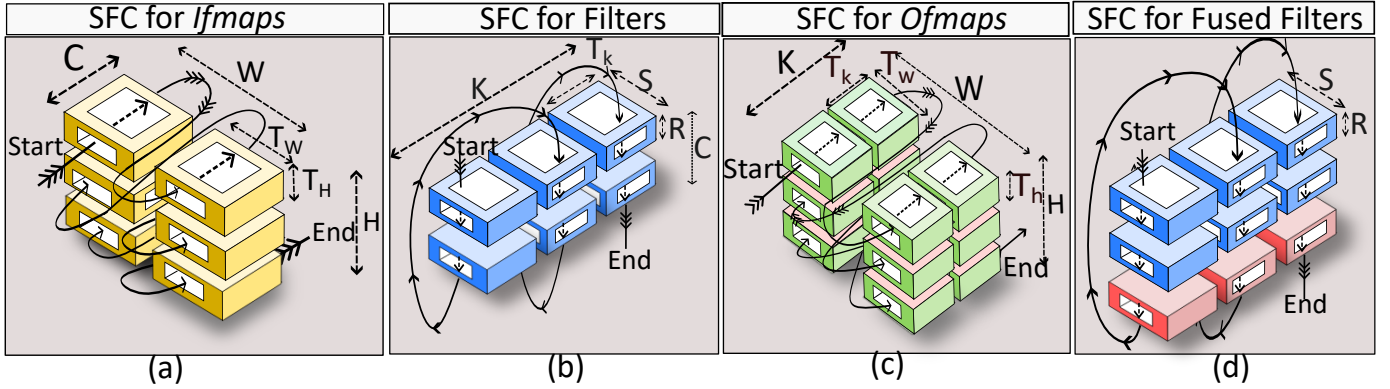


Fig. 8: SFCs (a) Reading *ifmaps*; (b) Reading the filters in a layer; (c) Writing *ofmaps*; (d) Reading fused filters across two layers

to unroll the weights. For instance, consider partitioning the weights into two sets: \mathcal{W}_1 and \mathcal{W}_2 . We create an unrolled SFC of the form $\mathcal{W}_1\mathcal{W}_2\mathcal{W}_1\mathcal{W}_2\dots$. To save space, we can perform limited unrolling, where if we need to read the weights τ times, we set the unrolling factor to η (model-specific secret). In extreme cases, we can have a situation where a deep tile does not fit in the NPU’s on-chip memory; this case can be solved by writing to multiple small SFCs and reading them in an interleaved fashion in the next layer. **Note that in all cases, the partitioning factor is a random variable that is generated in the same fashion as N**

C. Dealing with Halo Pixels

Halo pixels [58] are the additional pixels that are required to compute the convolution results in a tile (beyond its boundaries). In Figure 9, the halo pixels will be towards the north and west. Let the processing begin at the Northwest

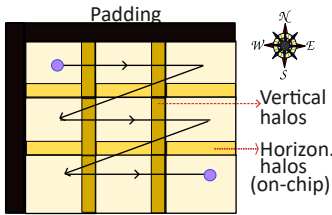


Fig. 9: Halo pixels in a layer

corner. We then proceed along the same row (towards East). Each tile in the northernmost row get its halo pixels from its western neighbor that has already been read. These pixels can be stored in a small on-chip buffer for immediate use. The number of halo pixels is quite small as compared to the sizes of the tiles. We proceed till we reach the last element of the row (eastern most). We then start at the westernmost column of the next row, and proceed eastward. In this case, the halo pixels need to come from the western neighbor and northern neighbor. The western neighbor (tile) was just read, however the northern neighbor (tile) was a part of the previous row. The first option is to store all the halo pixels in an on-chip buffer. In this case, when we are processing a row, we need

to store the halo pixels for the southern neighbors in an on-chip buffer. However, if there are space overflows, then we can write them as an SFC, and read them back in the same order when we are processing the next row.

D. Adding Custom Noise

The uncertainty in the number of tiles in each bin is integral to maintaining the overall security of the design as it obfuscates the *total data volume* and the *RW distance*. In $CX + N$, C naturally arises from compression and it can further be augmented with adding random dummy data [22], [50]. The additive noise $N = \alpha + N'$ can be added by keeping N bytes empty within a bin. For computing N' , we sample it from a heteroskedastic noise distribution, which makes the adversary’s job even harder. This distribution is characterized by its non-deterministic variance. This makes any kind of regression-based analysis hard. We performed the White [71] and Breusch-Pagan [5] tests using different combinations of distributions and estimated that a strong heteroskedastic noise distribution can be generated using a combination of the uniform and Gaussian distributions – both have very efficient hardware implementations [35], [43], [67], [68]. We use the uniform distribution (choice supported by Figure 6) to set the variance of the Gaussian distribution.

E. Layer Splitting and Fusion

In our architecture, performing layer splitting [38] and fusion are easy. In layer splitting, we partition an *ifmap* and assign each part to a sub-layer. In this case, the input SFC will be read once but the weight SFC may be read multiple times. We need to adopt the solution proposed in Case III. For layer fusion, we can split the *ifmap* if there is an on-chip space issue. Then for each set of deep tiles, we need to read the filters for two consecutive layers one after the other (Figure 8(d) shows how the filters are fused). For handling issues concerning limited on-chip storage, we can adopt the solutions for Cases II and III.

F. Pooling, ReLU and Skip Connections

The pooling and ReLU operations can be performed along with the convolution layer. Note that the tile size will change if we are pooling. If we are replacing a pixel with the maximum value in a window of 4 pixels, then the tile size will reduce by a factor of 4. In case, the tile size reduces to a very small value (let’s say 1×1), then we assume enough buffer space to read a large part of the input, recreate tiles, compress and place them into bins. Our design can easily handle skip connections as well – it simply requires re-reading the SFC of a previous layer. This will convey to the adversary that a skip connection exists (limitation in our design), however because of layer-boundary obfuscation, finding the source of the skip connection will be hard.

VI. PERFORMANCE EVALUATION

A. Setup and Benchmarks

Our experimental setup integrates the state-of-the-art DNN modeling tool (*Timeloop* [52]) and a cycle-accurate DRAM simulator (*Ramulator*). Both the simulators have been validated against real-world HW and are widely used in the literature. *Timeloop* [52] takes as input the details of the workload, the target NPU’s configuration (see Table IV), and the data reuse strategy as the input and generates performance statistics and traces.

We developed an in-house trace generator tool that extracts the memory access patterns of tiles from *Timeloop*’s T-traces [51] and then compresses and randomizes the tiles in accordance with our compression and binning strategies. Then, the tool generates a new sequence of memory accesses corresponding to bins. *Ramulator* takes traces from our trace generator tool as its input and generates the performance statistics.

Parameter	Value	Parameter	Value
PE size	16×12	Comp. buffer	182 kB
PE register	440 B	Global buffer	182 kB
DRAM	DDR3	Frequency	1.6 GHz

TABLE IV: Configuration of the NPU

Workloads We consider a set of dense as well sparse NN workloads (same as [9], [38], [74]). We generated pruned NNs using the layer-adaptive magnitude-based pruning technique [36] with a fairly good prediction accuracy as shown in Table V. Note that *NeuroPlug* will work for all types of convolution-based DNNs such as GANs and Transformers) since other basic layers such as the fully-connected layer can be easily expressed as a convolution [62]. We are not showing the results for Transformers and LLMs due to a paucity of space. Their sizes are huge and mounting a physical attack to estimate the model parameters is very

Model	Acc.
Pretrained	
<i>ResNet18</i> [25]	89.1%
<i>Vgg16</i> [63]	91.32%
<i>AlexNet</i> [33]	81%
Pruned	
<i>ResNet18</i> [25]	92.1%
<i>Vgg16</i> [63]	90%
<i>AlexNet</i> [33]	80%

TABLE V: Workloads

hard (massive search space). The

main target of such attacks are smaller DNNs.

We use an NVIDIA Tesla T4 GPU with CUDA 12.1 to train and prune the NN models using the CIFAR-10 dataset. We achieved an average accuracy of 90% for *Vgg16*, 80% for *Alexnet* and 92.1% for *ResNet18* – same as the original authors. During our analysis, we observed that many other popular CNN models demonstrated a similar behavior (not discussed due to paucity of space).

Configurations We select an unsecure system as the *baseline* configuration. The bin size was set to 60 kB. The TCB can store three bins at a time. We observed that the tile size varied with the layers and was roughly between 10 kB - 95 kB. We assume that an adversary analyzes the compression ratio (β) using other sister DNNs and crafts bespoke inputs; she observes that the values are normally distributed in the range $1.5 - 40\times$ [23] (also seen in our experiments). The *Compr* design represents a two-level compression (pruning [36] followed by *Huffman* compression) similar to the Deep Compression Algorithm [23]. The other configurations are – *DNNCloak* (*DNNCloak*) [9], Layer deepening (*NeuroObf_1*) [38], Layer widening (*NeuroObf_2*) [38], and Kernel widening (*NeuroObf_3*) [38]. In *NeuroPlug*, for the given set of models, the upper limit of the heteroskedastic noise distribution α was set to 8000 (in bytes).

B. Performance Analysis

The performance results are shown in Figure 10. The *performance* is proportional to the reciprocal of the total *#simulation cycles*. The results are normalized relative to the baseline setup. We find that *Compr* is $2.52\times$ faster than the baseline. This is due to the fact that compression leads to a reduction in memory traffic by a factor of $2.52\times$ as shown in Figure 11. There is a good correlation between performance and DRAM traffic, which is aligned with the findings reported in prior studies (*TNPU* [37], *Securator* [62], *GuardNN* [28]).

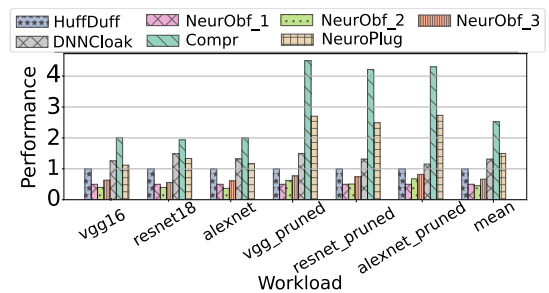


Fig. 10: Normalized performance

We see that on an average, the rest of the proposals [38] are $1.8\times$ worse than *NeuroPlug* in terms of performance. Note that *DNNCloak* performs *only* weight compression and incorporates an on-chip buffer to store the *ofmaps*, thereby reducing the memory traffic. But, it also includes dummy accesses and reads/writes the previous sublayer, which lead to an increase in the memory traffic, resulting in *DNNCloak* being 15.48% slower than *NeuroPlug*. On the contrary, *NeuroPlug* employs

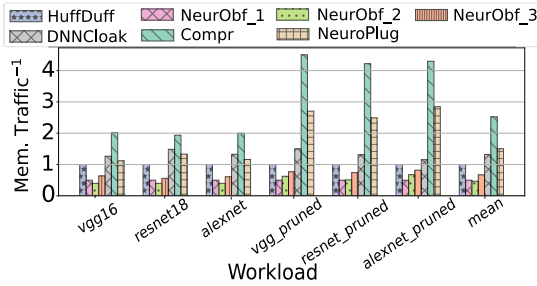


Fig. 11: Normalized memory traffic

compression to reduce all the off-chip communication, which allows us to afford more dummy accesses.

C. Sensitivity Analysis

Figure 12 shows the variation in the smart search space with the noise level (α) for *NeuroPlug*. The smart search space for *ResNet* is of the order of 10^{196} , for *Vgg16* is of the order of 10^{70} and for *AlexNet*, it is of the order of 10^{26} (small network, deliberately chosen).

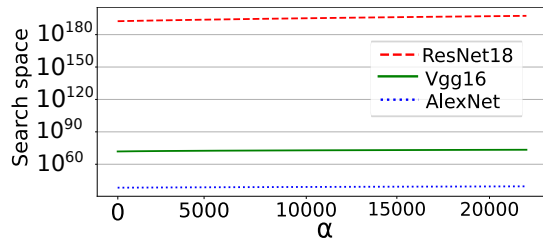


Fig. 12: Noise sensitivity analysis

Figure 13 shows the trade-off between the search space size and the performance overheads introduced by modulating C (adding random values).

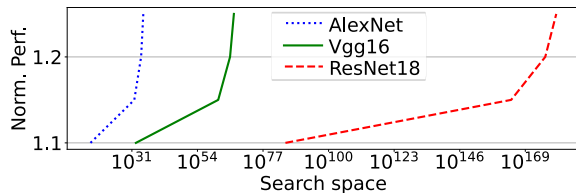


Fig. 13: Performance overhead vs search space size (► overheads increase very gradually)

D. Hardware Overheads

NeuroPlug incorporates additional HW, which can be added to conventional NPUs. The code for all the additional components was written in Verilog, and the designs were fully synthesized, placed, and routed using the Cadence Genus tool for a 28 nm ASIC technology node at 400 MHz frequency. We present the results in Table VI. Our design is generic and can work with any NPU (that works at the tile level) subject to making minimal changes. We show the results for an NPU that

Module	Area($\mu m^2 \times 10^3$)	Power(mW)
Compr-ency. engines	767	97.92
SFC addr. generator	8.35	0.56
Binning logic	1.26	1.47
Noise generator	3.29	0.340
Overall overhead (including buffers)	1581.40	130.43
Tool	Cadence RTL compiler, 28 nm	

TABLE VI: ASIC area and power utilization for the additional hardware components used in *NeuroPlug*

is based on the Eyeriss-2 accelerator [11] (its area is $5.5mm^2$).

We also implemented the design on a Virtex-7 FPGA board (xc7vx330t-3fg1157). The number of LUTs, registers and DRAMs required to implement the additional logic are 84K, 77K and 8 (resp.) at a frequency of 360 MHz.

VII. SECURITY EVALUATION

We perform a thorough security analysis using multiple DNNs. We primarily report the results for the *Vgg16* model, which is more vulnerable to attacks because of its lack of skip connections, good accuracy, and relatively small model size that reduce the search space. The results for other NNs are similar or better (not presented due to space constraints).

A. Search Space Sensitivity

We estimate the variation in the smart search space size as shown in Figure 14 with different noise levels. We vary the level of the noise α in the presence and absence of compression – $Y = \beta X + \alpha$. Here β is the ratio of the size of the compressed data and the size of the original data. We observe that with the same level of noise(α), the search space of $Y = \beta X + \alpha$ is of the order 10^{70} , while for $Y = X + \alpha$, it is of the order 10^{26} (significantly smaller).

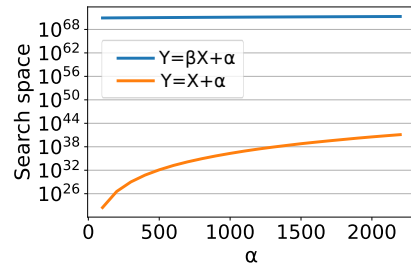


Fig. 14: Variation in the smart search space size with and without compression (VGG16). **Conclusion:** compression is needed.

We also mount an attack in the presence of *NeuroPlug* and report the accuracy of the *top* nine models in CIFAR-10 that can be estimated by the adversary in Figure 15. These accuracies are similar to the accuracy of a randomly generated model (10 – 20%), where no leakage hints are available.

Next, we perform two distinct case studies to examine the security of our scheme against two highly potent recent attacks: *HuffDuff* [74] and *Reverse Engg* [29]. There is no

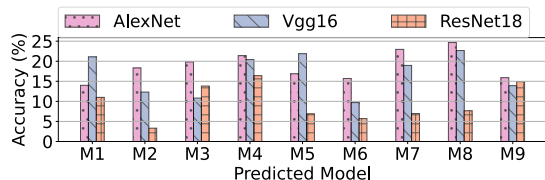


Fig. 15: Accuracy of the models estimated by an attacker

known countermeasure for HuffDuff. A total of 2048 unique memory traffic traces were collected using various inputs (as in the *HuffDuff* model) in order to perform the security analysis for the *Vgg16* model. Note that the conclusions for other DNNs, such as *ResNet18* and *AlexNet*, are identical (not presented due to space constraints).

B. Case Study 1 – Defense from HuffDuff

We analyze the first five most vulnerable layers of the *Vgg16* model across three distinct configurations – scheme without any CM, our proposed scheme (*NeuroPlug*) as the CM, and a hypothetical secure system *random* that provides complete security guarantees, ensuring that any data observed by an adversary is entirely random and unrelated to the architecture of the models. Other competing CMs are not considered since they cannot stop this attack. We employ a combination of information-theory and statistics-based tests to assess the security of *NeuroPlug*. This approach is favored in the cryptography community as it avoids reliance on a single metric. For example, the classical correlation coefficient could be zero for random variables x and x^2 , however, other security metrics reveal their underlying connection.

Information Theoretic Tests - We use FI (Fisher Information) and MI (Mutual Information), which are extensively used metrics to estimate the information content of leaked signatures and their association with secret data/keys [8], [14], [18]–[20], [24], [31], [42], [46], [54]. **These metrics can never be zero for a distribution with a finite support. Our aim is to bring them as close to the random configuration as possible.**

► *Fisher information (FI)* The FI is a robust and classical method for establishing a lower bound on the error (variance) of the estimator – the lower the better [42]. We mount the *HuffDuff* attack and observe that the FI is quite low for the first 5 layers (comparable to random). It reduces as we consider deeper layers (due to epistemic uncertainty).

HuffDuff relies on the information distortion (number of non-zero (NNZ) values) at the edges of an *fmap* due to the way the convolution operation handles the edge pixels. This discrepancy decreases with the layer depth as shown in Figure 16. The FI in Figure 17 validates the same fact. A similar behavior was observed in all the other layers and NNs. Note how close our FI is to a truly random source (within 6%).

► *Mutual information (MI)* We estimate the MI between the leaked traces and the hidden parameter (filter size) for all the three configurations. We observe a similar pattern here, indicating that the amount of *information between the hidden parameter and the leaked traces for NeuroPlug is nearly the*

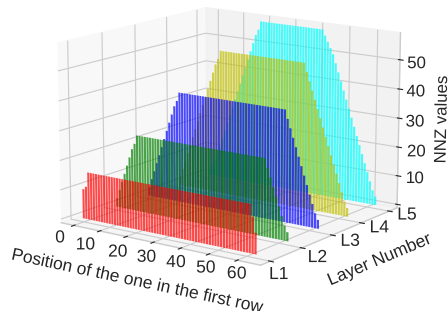


Fig. 16: The boundary effect decreases with the layer depth. 64 different 64×64 inputs are created by varying the position of the one in the first row of the input with all zeros.

same as the information between random data and the hidden parameter.

Statistical Tests We perform the runs test [2] (part of the NIST suite [44]) and CVM tests [12], which are considered as the standard approaches to quantify security.

► *Runs test* The average p -value for *NeuroPlug* is 0.41, which is more (better) than the standard threshold value of 0.05 (corresponding to the null hypothesis). This establishes the random nature of the source as per this test.

► *Cramer–von Mises (CVM) test* [3], [12], [17] We estimate the *CVM distance*, which decreases as the difference between the random data and the sampled data decreases. We observe that *NeuroPlug* exhibits the lowest CVM (closest to random, see Figure 17).

► *Correlation coefficient (CC)* We calculate the classical CC to estimate the degree of correlation between the leaked signal and the hidden parameter using *Pearson’s CC* (see Figure 17). Here also we have make a similar inference.

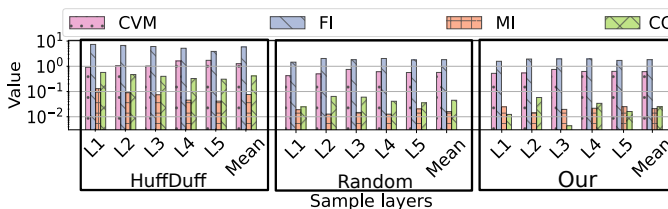


Fig. 17: Security analyses for Case Study 1. *MI* is b/w the secret parameter and the leaked metric. *CC* is b/w the leaked traces and the filter size.

C. Case Study 2 – Defense from Reverse Engg.

We implemented *ReverseEngg* [29], which is a state-of-the-art memory-based SCA (side-channel attack) that steals the model architecture in the absence of any CMs; it is the basis for many other attacks that use the same principle such as [27], [73]. We implemented two CMs (based on this): (*NeurObfuscator* [38] and *DNNcloak* [9]) – the former introduces dummy computations and the latter uses a combination of dummy accesses, partial encryption and extensive on-chip buffering. We compute the distribution for the two

most important architectural hints (exposed via side channels): RW distance and the total traffic distribution (see Table VII). We observe minimal differences in the FI between *NeuroPlug* and *DNNCloak* indicating that both the schemes are effective at mitigating address-based SCAs. However, *DNNCloak* can be broken using timing and Kerckhoff-based attacks (see Section III-2), whereas *NeuroPlug* is immune to them.

Scheme	MI	CC	FI	MI	CC	FI
	Memory traffic			RW distance		
<i>NeurObfu.</i>	0.898	0.959	0.658	0.859	0.807	1.9
<i>DNNCloak</i>	0.846	0.923	0.038	0.635	0.781	0.236
<i>Random</i>	0.234	0.211	0.123	0.324	0.298	0.430
<i>NeuroPlug</i>	0.436	0.243	0.057	0.456	0.289	0.222

TABLE VII: Security analysis for Case Study 2

VIII. RELATED WORK

A. DNN Architecture Extraction: CDTV Metrics

Table VIII shows a summary of the most popular DNN architecture stealing attacks. Hua et al. [29] propose a state-of-the-art attack, which builds constraint equations by observing memory access patterns and the traffic volume. Similarly, DeepSniffer [27] exploits the relationship between architectural hints such as memory reads/write volumes and a DNN’s architecture. The authors of HuffDuff [74] exploit the *boundary effect* and the timing side-channel for attacking sparse CNN accelerators. The boundary effect occurs at the outermost edge of a convolution layer where we perform fewer multiplications – this helps the attacker discern filter dimensions. Cache Telepathy [73] steals the CNN’s architecture by estimating the timing information using cache-based prime-probe attack. They use this information to infer the total number of calls for performing multiplication, which helps estimate the model architecture.

Attack	Theft target		Leaked Metric			
	Arch.	Params	C	D	T	V
ReverseEngg [29]	●	●	○	●	○	●
CacheTelepathy [73]	●	○	●	●	●	●
DeepSniffer [27]	●	○	○	●	○	●
HuffDuff [74]	●	○	○	●	●	●

TABLE VIII: Different Attacks on NNs. (C,D,T,V) stands for (Count, Distance, Time, Volume)

B. DNN Architecture Protection

1) *Shuffling-based CMs*: Liu et al. [40] proposed to shuffle the addresses, while Li et al. [38] obscured the tile access pattern by shuffling the order of the tile accesses. Sadly, their scheme still preserves counts and average RW distances [9]. Additionally, shuffling requires a huge mapping table that is hard to store on chip. [9].

2) *Redundancy-based CMs*: The number of memory accesses or the process execution time information can be hidden by incorporating dummy memory accesses or by adding delays.

► *Redundancy in Space* Li et al. [38] employ different obfuscation techniques such as layer deepening and kernel widening that introduce dummy memory accesses. This makes it necessary to read all the dummy data at least once during the execution of the DNN, and then use or hide the results. Che et al. [9] emphasize that attackers can distinguish between layer types by examining memory access intensities. They suggest adding dummy accesses to equalize the number of accesses across the layers, which leads to high performance overheads. The CDTV information is nonetheless available.

► *Redundancy in Time* Wang et al. propose *NPUFort* [70] – a custom HW accelerator that encrypts only security-critical features. Sadly, partial encryption of the weights only provides partial security. Similarly, cache-telepathy [73] proposes to run an entire toy NN to obfuscate the timing information of the DNN – this still ends up exposing a lot of CDV information (much more than the state of the art CMs).

3) *Access Removal using On-Chip Buffering*: Che et al. [9] choose to buffer a part of the *ofmap* due to which an adversary will find it difficult to infer the size of the *ofmap* (can be broken using schemes shown in Section II).

IX. DISCUSSION AND CONCLUSION

The key contribution of this paper is as follows. Assume a threat model where an adversary can **observe** all the addresses being sent to encrypted, tamper-proof DRAM memory, and **record** the volume of encrypted data transferred as well as the associated timing information. All known attacks and CMs on NNs use a subset of the CDTV metrics. We are not aware of any fifth metric that can be derived from an observation of DRAM accesses and timing, which is fundamentally different. In the backdrop of this observation, we create a comprehensive universal attack that relies on a combination of SS, KK and SI attacks to break all state-of-the-art CMs in 8-10 hours on current machines. The primary deficiency of current CMs is that they rely on additive noise, hardware parameters that can be leaked by malicious insiders and do not take cognizance of the side-information available to an adversary. *NeuroPlug* is a novel CM that prevents SS, KK and SI attacks using CDTV metrics in the context of the aforementioned threat model. Its cornerstone is the addition of multiplicative noise of the form $Y = CX + N$, where the factor C arises naturally from feature map compression. This formulation inherently leads to a mathematical framework based on Mellin transforms where the search space size can be precisely quantified. Its size can further be increased by modulating C (adding random data to layers) depending on the model creator’s requirements.

This multiplicative formulation naturally leads to a design that represents the 3D computation in a CNN as a read-once-write-once 1D computation using SFCs (novel contribution). We further show that all kinds of corner cases including handling halo pixels and weights that do not fit in on-chip memory can be easily handled using our SFC-based framework. All the proposed HW structures were meticulously coded in Verilog and synthesized for two targets: 28-nm ASIC process and the

Virtex-7 FPGA. The HW overheads are quite modest (1.5 mm^2 on the ASIC).

Our design has a large search space size (10^{196} for *ResNet18* and 10^{70} for *Vgg16*) with a minimal performance degradation with respect to the unsecure baseline. Moreover, for all the known statistical tests (also part of the NIST test suite), the information leaked by *NeuroPlug* is statistically very similar to a truly random source for the CDTV metrics, even in the presence of specially crafted inputs (Case Studies 1 and 2). With a minimal loss in performance, it is possible to substantially increase the search space size (e.g. multiply it by 10^{50}) by modulating the multiplicative parameter. Owing to compression, which is intrinsically aligned with our SFC-based framework, we note a performance improvement of 15.48% over our nearest competitor DNNcloak [9].

REFERENCES

- [1] "Asml claims an employee stole chip manufacturing secrets and sold them to china," 2023, accessed on 3 April, 2024. [Online]. Available: <https://www.firstpost.com/world/asml-claims-an-employee-stole-chip-manufacturing-secrets-and-sold-them-to-china-12170742.html>
- [2] M. A. Agin and A. P. Godbole, "A new exact runs test for randomness," in *Computing Science and Statistics: Statistics of Many Parameters: Curves, Images, Spatial Models*. Springer, 1992, pp. 281–285.
- [3] L. Baringhaus and N. Henze, "Cramér–von mises distance: probabilistic interpretation, confidence intervals, and neighbourhood-of-model validation," *Journal of Nonparametric Statistics*, vol. 29, no. 2, pp. 167–188, 2017.
- [4] J. Bertrand, P. Bertrand, and J.-P. Ovarlez, "The mellin transform," 1995.
- [5] T. S. Breusch and A. R. Pagan, "A simple test for heteroscedasticity and random coefficient variation," *Econometrica: Journal of the econometric society*, pp. 1287–1294, 1979.
- [6] I. A. Canales-Martínez, J. Chávez-Saab, A. Hambitzer, F. Rodríguez-Henríquez, N. Satpute, and A. Shamir, "Polynomial time cryptanalytic extraction of neural network models," in *Annual International Conference on the Theory and Applications of Cryptographic Techniques*. Springer, 2024, pp. 3–33.
- [7] N. Carlini, M. Jagielski, and I. Mironov, "Cryptanalytic extraction of neural network models," in *Annual international cryptology conference*. Springer, 2020, pp. 189–218.
- [8] K. Chatzikokolakis, T. Chothia, and A. Guha, "Statistical measurement of information leakage," in *International Conference on Tools and Algorithms for the Construction and Analysis of Systems*. Springer, 2010, pp. 390–404.
- [9] Y. Che and R. Wang, "Dnncloak: Secure dnn models against memory side-channel based reverse engineering attacks," in *2022 IEEE 40th International Conference on Computer Design (ICCD)*. IEEE, 2022, pp. 89–96.
- [10] J. Chen, L. Chen, and Y. Zhou, "Cryptanalysis of image ciphers with permutation-substitution network and chaos," *IEEE Transactions on Circuits and Systems for Video Technology*, vol. 31, no. 6, pp. 2494–2508, 2020.
- [11] Y.-H. Chen, T.-J. Yang, J. Emer, and V. Sze, "Eyeriss v2: A flexible accelerator for emerging deep neural networks on mobile devices," *IEEE Journal on Emerging and Selected Topics in Circuits and Systems*, vol. 9, no. 2, pp. 292–308, 2019.
- [12] V. Choulakian, R. A. Lockhart, and M. A. Stephens, "Cramér-von mises statistics for discrete distributions," *The Canadian Journal of Statistics/La Revue Canadienne de Statistique*, pp. 125–137, 1994.
- [13] V. Costan and S. Devadas, "Intel sgx explained," in *Cryptology ePrint Archive, TechnicalReport086, MIT*, 2016.
- [14] V. Cristiani, M. Lecomte, and P. Maurine, "Leakage assessment through neural estimation of the mutual information," in *Applied Cryptography and Network Security Workshops: ACNS 2020 Satellite Workshops, AIBlock, AIHWS, AIoTS, Cloud S&P, SCI, SecMT, and SiMLA, Rome, Italy, October 19–22, 2020, Proceedings 18*. Springer, 2020, pp. 144–162.
- [15] A. De Sena and D. Rocchesso, "A fast mellin and scale transform," *EURASIP Journal on Advances in Signal Processing*, vol. 2007, pp. 1–9, 2007.
- [16] S. Dhall, S. K. Pal, and K. Sharma, "Cryptanalysis of image encryption scheme based on a new 1d chaotic system," *Signal processing*, vol. 146, pp. 22–32, 2018.
- [17] C. Dowd, "A new ecdf two-sample test statistic," *arXiv preprint arXiv:2007.01360*, 2020.
- [18] A. Duc, S. Faust, and F.-X. Standaert, "Making masking security proofs concrete: or how to evaluate the security of any leaking device," in *Advances in Cryptology—EUROCRYPT 2015: 34th Annual International Conference on the Theory and Applications of Cryptographic Techniques, Sofia, Bulgaria, April 26–30, 2015, Proceedings, Part 1 34*. Springer, 2015, pp. 401–429.
- [19] F. Farokhi and M. A. Kaafar, "Modelling and quantifying membership information leakage in machine learning," *arXiv preprint arXiv:2001.10648*, 2020.
- [20] T. Filler and J. Fridrich, "Fisher information determines capacity of ϵ -secure steganography," in *International Workshop on Information Hiding*. Springer, 2009, pp. 31–47.
- [21] J. Gawlikowski, C. R. N. Tassi, M. Ali, J. Lee, M. Humt, J. Feng, A. Kruspe, R. Triebel, P. Jung, R. Roscher *et al.*, "A survey of uncertainty in deep neural networks," *Artificial Intelligence Review*, vol. 56, no. Suppl 1, pp. 1513–1589, 2023.
- [22] Q. Geng and P. Viswanath, "Optimal noise adding mechanisms for approximate differential privacy," *IEEE Transactions on Information Theory*, vol. 62, no. 2, pp. 952–969, 2015.
- [23] S. Han, H. Mao, and W. J. Dally, "Deep quantization: Compressing deep neural networks with pruning, trained quantization and Huffman coding," *arXiv preprint arXiv:1510.00149*, 2015.
- [24] A. Hannun, C. Guo, and L. van der Maaten, "Measuring data leakage in machine-learning models with fisher information," in *Uncertainty in Artificial Intelligence*. PMLR, 2021, pp. 760–770.
- [25] K. He, X. Zhang, S. Ren, and J. Sun, "Deep residual learning for image recognition," in *Proceedings of the IEEE conference on computer vision and pattern recognition*, 2016, pp. 770–778.
- [26] A. G. Howard, M. Zhu, B. Chen, D. Kalenichenko, W. Wang, T. Weyand, M. Andreetto, and H. Adam, "Mobilenets: Efficient convolutional neural networks for mobile vision applications," *arXiv preprint arXiv:1704.04861*, 2017.
- [27] X. Hu, L. Liang, S. Li, L. Deng, P. Zuo, Y. Ji, X. Xie, Y. Ding, C. Liu, T. Sherwood *et al.*, "Deepsniffer: A dnn model extraction framework based on learning architectural hints," in *Proceedings of the Twenty-Fifth International Conference on Architectural Support for Programming Languages and Operating Systems*, 2020, pp. 385–399.
- [28] W. Hua, M. Umar, Z. Zhang, and G. E. Suh, "Guardnn: secure accelerator architecture for privacy-preserving deep learning," in *Proceedings of the 59th ACM/IEEE Design Automation Conference*, 2022, pp. 349–354.
- [29] W. Hua, Z. Zhang, and G. E. Suh, "Reverse engineering convolutional neural networks through side-channel information leaks," in *Proceedings of the 55th Annual Design Automation Conference*, 2018, pp. 1–6.
- [30] F. N. Iandola, S. Han, M. W. Moskewicz, K. Ashraf, W. J. Dally, and K. Keutzer, "Squeezenet: Alexnet-level accuracy with 50x fewer parameters and 0.5 mb model size," *arXiv preprint arXiv:1602.07360*, 2016.
- [31] A. Keramat, M. S. Ghidaoui, X. Wang, and M. Louati, "Cramer-rao lower bound for performance analysis of leak detection," *Journal of Hydraulic Engineering*, vol. 145, no. 6, p. 04019018, 2019.
- [32] T. Knoll, "Adapting kerckhoffs's principle," *Advanced Microkernel Operating Systems (2018)*, vol. 93, 2018.
- [33] A. Krizhevsky, I. Sutskever, and G. E. Hinton, "Imagenet classification with deep convolutional neural networks," *Advances in neural information processing systems*, vol. 25, 2012.
- [34] S. Kumar, A. Panda, and S. R. Sarangi, "Securelease: Maintaining execution control in the wild using intel sgx," in *Proceedings of the 23rd ACM/IFIP International Middleware Conference*, 2022, pp. 29–42.
- [35] D.-U. Lee, W. Luk, J. D. Villasenor, and P. Y. Cheung, "A gaussian noise generator for hardware-based simulations," *IEEE Transactions on Computers*, vol. 53, no. 12, pp. 1523–1534, 2004.
- [36] J. Lee, S. Park, S. Mo, S. Ahn, and J. Shin, "Layer-adaptive sparsity for the magnitude-based pruning," in *International Conference on Learning Representations*, 2021. [Online]. Available: <https://openreview.net/forum?id=H6ATjJOTKdf>

- [37] S. Lee, J. Kim, S. Na, J. Park, and J. Huh, "Tnpu: Supporting trusted execution with tree-less integrity protection for neural processing unit," in *2022 IEEE International Symposium on High-Performance Computer Architecture (HPCA)*. IEEE, 2022, pp. 229–243.
- [38] J. Li, Z. He, A. S. Rakin, D. Fan, and C. Chakrabarti, "Neurobfuscator: A full-stack obfuscation tool to mitigate neural architecture stealing," in *2021 IEEE International Symposium on Hardware Oriented Security and Trust (HOST)*. IEEE, 2021, pp. 248–258.
- [39] Y. Liu, X. Chen, C. Liu, and D. Song, "Delving into transferable adversarial examples and black-box attacks," *arXiv preprint arXiv:1611.02770*, 2016.
- [40] Y. Liu, D. Dachman-Soled, and A. Srivastava, "Mitigating reverse engineering attacks on deep neural networks," in *2019 IEEE Computer Society Annual Symposium on VLSI (ISVLSI)*. IEEE, 2019, pp. 657–662.
- [41] Y. Long, V. Bindschaedler, L. Wang, D. Bu, X. Wang, H. Tang, C. A. Gunter, and K. Chen, "Understanding membership inferences on well-generalized learning models," *arXiv preprint arXiv:1802.04889*, 2018.
- [42] K. Maeng, C. Guo, S. Kariyappa, and E. Suh, "Measuring and controlling split layer privacy leakage using fisher information," *arXiv preprint arXiv:2209.10119*, 2022.
- [43] J. S. Malik and A. Hemani, "Gaussian random number generation: A survey on hardware architectures," *ACM Computing Surveys (CSUR)*, vol. 49, no. 3, pp. 1–37, 2016.
- [44] K. Marton and A. Suciú, "On the interpretation of results from the nist statistical test suite," *Science and Technology*, vol. 18, no. 1, pp. 18–32, 2015.
- [45] J. L. Massey, "Guessing and entropy," in *Proceedings of 1994 IEEE International Symposium on Information Theory*. IEEE, 1994, p. 204.
- [46] A. L. Mayer, C. W. Pawlowski, and H. Cabezas, "Fisher information and dynamic regime changes in ecological systems," *Ecological modelling*, vol. 195, no. 1-2, pp. 72–82, 2006.
- [47] T. McGrath, I. E. Bagci, Z. M. Wang, U. Roedig, and R. J. Young, "A puf taxonomy," *Applied physics reviews*, vol. 6, no. 1, 2019.
- [48] G. Mincu and L. Panaïopol, "On some properties of squarefree and squareful numbers," *Bulletin mathématique de la Société des Sciences Mathématiques de Roumanie*, pp. 63–68, 2006.
- [49] N. Morgulis, A. Kreines, S. Mendelowitz, and Y. Weisglass, "Fooling a real car with adversarial traffic signs," *arXiv preprint arXiv:1907.00374*, 2019.
- [50] K. Nissim, S. Raskhodnikova, and A. Smith, "Smooth sensitivity and sampling in private data analysis," in *Proceedings of the thirty-ninth annual ACM symposium on Theory of computing*, 2007, pp. 75–84.
- [51] A. Parashar, P. Chatarasi, and P.-A. Tsai, "Hardware abstractions for targeting eddo architectures with the polyhedral model," in *11th International Workshop on Polyhedral Compilation Techniques (Vital Event)(IMPACT 2021)*, 2021.
- [52] A. Parashar, P. Raina, Y. S. Shao, Y.-H. Chen, V. A. Ying, A. Mukkara, R. Venkatesan, B. Khailany, S. W. Keckler, and J. Emer, "Timeloop: A systematic approach to dnn accelerator evaluation," in *2019 IEEE international symposium on performance analysis of systems and software (ISPASS)*. IEEE, 2019, pp. 304–315.
- [53] J. Paulson, "Data security in the age of supercomputing," Dec, 2023, accessed on 3 April, 2024. [Online]. Available: <https://medium.com/@cybertec/data-security-in-the-age-of-supercomputing-3b66464e54a0>
- [54] E. Prouff and M. Rivain, "Theoretical and practical aspects of mutual information based side channel analysis," in *Applied Cryptography and Network Security: 7th International Conference, ACNS 2009, Paris-Rocquencourt, France, June 2-5, 2009. Proceedings 7*. Springer, 2009, pp. 499–518.
- [55] L. Pryimenko, "Insider threats and their consequences," Feb, 2024, accessed on 3 April, 2024. [Online]. Available: <https://www.ekransystem.com/en/blog/real-life-examples-insider-threat-caused-breaches>
- [56] D. Ritchie, "Samsung ex-employees leak tech firm's dram secrets," 2023, accessed on 3 April, 2024. [Online]. Available: <https://readwrite.com/samsung-ex-employees-leak-tech-firms-dram-secrets/>
- [57] H. Sagan, "Hilbert's space-filling curve," in *Space-filling curves*. Springer, 1994, pp. 9–30.
- [58] S. R. Sarangi, *Next-Gen Computer Architecture*, 1st ed. White Falcon.
- [59] V. Scarlata, S. Johnson, J. Beaney, and P. Zmijewski, "Supporting third party attestation for intel sgx with intel data center attestation primitives," *White paper*, vol. 12, 2018.
- [60] A. Shilov, "Samsung fab workers leak confidential data while using chatgpt," April, 2023, accessed on 3 April, 2024. [Online]. Available: <https://www.tomshardware.com/news/samsung-fab-workers-leak-confidential-data-to-chatgpt>
- [61] N. Shrivastava et al., "Scedl: A simultaneous compression and encryption scheme for deep learning models," 2023.
- [62] N. Shrivastava and S. R. Sarangi, "Securator: A fast and secure neural processing unit," in *2023 IEEE International Symposium on High-Performance Computer Architecture (HPCA)*. IEEE, 2023, pp. 1127–1139.
- [63] K. Simonyan and A. Zisserman, "Very deep convolutional networks for large-scale image recognition," *arXiv preprint arXiv:1409.1556*, 2014.
- [64] Y. Song, Z. Zhu, W. Zhang, H. Yu, and Y. Zhao, "Efficient and secure image encryption algorithm using a novel key-substitution architecture," *IEEE Access*, vol. 7, pp. 84 386–84 400, 2019.
- [65] C. Szegedy, W. Liu, Y. Jia, P. Sermanet, S. Reed, D. Anguelov, D. Erhan, V. Vanhoucke, and A. Rabinovich, "Going deeper with convolutions," in *Proceedings of the IEEE conference on computer vision and pattern recognition*, 2015, pp. 1–9.
- [66] C. Szegedy, V. Vanhoucke, S. Ioffe, J. Shlens, and Z. Wojna, "Rethinking the inception architecture for computer vision," in *Proceedings of the IEEE conference on computer vision and pattern recognition*, 2016, pp. 2818–2826.
- [67] D. B. Thomas and W. Luk, "Fpga-optimised uniform random number generators using luts and shift registers," in *2010 International Conference on Field Programmable Logic and Applications*. IEEE, 2010, pp. 77–82.
- [68] D. B. Thomas and W. Luk, "The lut-sr family of uniform random number generators for fpga architectures," *IEEE transactions on very large scale integration (vlsi) systems*, vol. 21, no. 4, pp. 761–770, 2012.
- [69] M. Wan, M. Han, L. Li, Z. Li, and S. He, "Effects of and defenses against adversarial attacks on a traffic light classification cnn," in *Proceedings of the 2020 ACM Southeast Conference*, 2020, pp. 94–99.
- [70] X. Wang, R. Hou, Y. Zhu, J. Zhang, and D. Meng, "Npufort: A secure architecture of dnn accelerator against model inversion attack," in *Proceedings of the 16th ACM International Conference on Computing Frontiers*, 2019, pp. 190–196.
- [71] H. White, "A heteroskedasticity-consistent covariance matrix estimator and a direct test for heteroskedasticity," *Econometrica: journal of the Econometric Society*, pp. 817–838, 1980.
- [72] F. Woitschek and G. Schneider, "Physical adversarial attacks on deep neural networks for traffic sign recognition: A feasibility study," in *2021 IEEE Intelligent vehicles symposium (IV)*. IEEE, 2021, pp. 481–487.
- [73] M. Yan, C. Fletcher, and J. Torrellas, "Cache telepathy: Leveraging shared resource attacks to learn dnn architectures," in *USENIX Security Symposium*, 2020.
- [74] D. Yang, P. J. Nair, and M. Lis, "Huffduff: Stealing pruned dnns from sparse accelerators," in *Proceedings of the 28th ACM International Conference on Architectural Support for Programming Languages and Operating Systems, Volume 2*, 2023, pp. 385–399.
- [75] F. Yao, A. S. Rakin, and D. Fan, "Deephammer: Depleting the intelligence of deep neural networks through targeted chain of bit flips," in *29th USENIX Security Symposium (USENIX Security 20)*, 2020, pp. 1463–1480.
- [76] M. Zeinali, S. Shahmorad, and K. Mirnia, "Hermite and piecewise cubic hermite interpolation of fuzzy data," *Journal of Intelligent & Fuzzy Systems*, vol. 26, no. 6, pp. 2889–2898, 2014.
- [77] X. Zhang, X. Zhou, M. Lin, and J. Sun, "Shufflenet: An extremely efficient convolutional neural network for mobile devices," in *Proceedings of the IEEE conference on computer vision and pattern recognition*, 2018, pp. 6848–6856.
- [78] T. Zhou, S. Ren, and X. Xu, "Obfunas: A neural architecture search-based dnn obfuscation approach," in *Proceedings of the 41st IEEE/ACM International Conference on Computer-Aided Design*, 2022, pp. 1–9.
- [79] V. Ziyadinov and M. Tereshonok, "Noise immunity and robustness study of image recognition using a convolutional neural network," *Sensors*, vol. 22, no. 3, p. 1241, 2022.
- [80] P. Zuo, Y. Hua, L. Liang, X. Xie, X. Hu, and Y. Xie, "Sealing neural network models in encrypted deep learning accelerators," in *2021 58th ACM/IEEE Design Automation Conference (DAC)*. IEEE, 2021, pp. 1255–1260.